

Salsolinol improves angiotensin II-induced myocardial fibrosis *in vitro* via inhibition of LSD1 through regulation of the STAT3/Notch-1 signaling pathway

XIAN ZHANG^{1,2}, ZE SHAO¹, YUCHAO NI¹, FEILONG CHEN¹, XIA YU¹ and JIASHENG WEN¹

¹Cardiology Department, Kunshan Hospital of Integrated Traditional Chinese and Western Medicine, Kunshan, Jiangsu 215332; ²Shandong University of Traditional Chinese Medicine, Jinan, Shandong 250014, P.R. China

Received February 21, 2023; Accepted July 3, 2023

DOI: 10.3892/etm.2023.12226

Abstract. The clinical incidence of congestive heart failure (CHF) is very high and it poses a significant threat to the health of patients. The traditional Chinese medicine monomer salsolinol is widely used to treat similar symptoms of CHF. However, there have been no reports on the effect of salsolinol for the management of CHF and its effects on myocardial fibrosis. In the present study, salsolinol was used to treat angiotensin II (AngII)-induced human cardiac fibroblasts (HCFs) and cell proliferation and migration were assessed using a CCK-8, EdU staining assay and wound healing assay. Subsequently, immunofluorescence, western blotting and other techniques were used to detect indicators associated with cell fibrosis and relevant kits were used to detect markers of cellular inflammation and reactive oxygen species (ROS) production. Molecular docking analysis was used to predict the relationship between salsolinol and lysine-specific histone demethylase 1A (LSD1). Subsequently, the expression of LSD1 in the serum of CHF patients was detected by reverse transcription-quantitative PCR. Finally, LSD1 was overexpressed in cells to explore the regulatory mechanism of salsolinol in AngII-induced HCFs. Salsolinol reduced the proliferation and migration. Salsolinol reduced the expression of fibrosis marker proteins α -smooth muscle actin, Collagen I and Collagen III in a concentration-dependent manner, thereby reducing cell fibrosis. In addition, salsolinol reduced the levels of TNF- α and IL-6 in the cell supernatant and ROS production following AngII induction. Salsolinol inhibited LSD1 expression and regulated the STAT3/Notch-1 signaling pathway. Upregulation of LSD1 reversed the effects of salsolinol on AngII-induced

HCFs. Salsolinol inhibited LSD1 via regulation of the STAT3/Notch-1 signaling pathway to improve Ang II-induced myocardial fibrosis *in vitro*.

Introduction

Congestive heart failure (CHF) refers to a series of clinical syndromes in which the systolic and diastolic function of the heart is seriously impaired by various pathogenic factors, resulting in a decline in the pumping function of the heart and the inability to expel blood to meet the metabolic needs of the body (1). The clinical incidence of CHF is high with a frequency of 1-2% of the population (2) and it poses a serious threat to the health of patients. Thus, there is an urgent need to identify novel therapeutic drugs.

Aconite was widely used in ancient China to treat similar symptoms of heart failure (3). A previous study showed that the combination of water-soluble alkaloids of aconite and total ginsenosides had a therapeutic effect in a rat model of acute heart rats (4). It can also inhibit apoptosis in rats with chronic heart failure (5). Salsolinol is the primary water-soluble heart-stimulating alkaloid of aconite and has a heart-stimulating strengthening effect similar to that of β -adrenalin. A previous study showed that salsolinol has analgesic, anti-inflammatory and heart-strengthening effects (6). Salsolinol alleviates doxorubicin-induced chronic heart failure in rats and improves mitochondrial function of H9C2 cardiomyocytes (7). However, the role of salsolinol in myocardial fibrosis and its mechanism have not been reported thus far. According to SwissTargetPrediction database (<http://www.swisstargetprediction.ch/>), lysine-specific demethylase 1 (LSD1; also known as KDM1A) is a potential target of salsolinol. LSD1, the first identified histone demethylase, serves an important role in embryonic development, epithelial-interstitial transformation, cell differentiation and tumor proliferation, invasion and metastasis (8). Inhibition of LSD1 in pregnant mice or neonatal mice prevents cardiomyopathy and LSD1 may be a therapeutic target for the prevention or treatment of dilated cardiomyopathy complicated with laminopathy (9). After 20 weeks of transverse aortic contraction, LSD1 expression increases not only in human dilated cardiomyopathic hearts but also in wild-type mouse heart homogenates and isolated cardiac fibroblasts (10).

Correspondence to: Dr Jiasheng Wen, Cardiology Department, Kunshan Hospital of Integrated Traditional Chinese and Western Medicine, 388 Jinrong Road, Kunshan, Jiangsu 215332, P.R. China
E-mail: wenjiasheng1126@163.com

Key words: congestive heart failure, salsolinol, myocardial fibrosis, lysine-specific histone demethylase 1A, STAT3/Notch-1 signaling pathway

In addition, upregulation of LSD1 is also observed in angiotensin II (Ang II)-treated neonatal rat myocardial fibroblasts and *in vivo* myoblast-specific LSD1 knockout significantly alleviated systolic dysfunction, myocardial hypertrophy and fibrosis at 6 and 20 weeks after transaortic contraction (10), which indicated that LSD1 might be a potential target for the treatment of heart failure. However, whether salsolinol serves a regulatory role in myocardial fibrosis through LSD1 has not been reported in the literature, to the best of the authors' knowledge.

The aim of the present study was to determine the effect of salsolinol in angiotensin II-induced myocardial fibrosis and ascertain the underlying mechanism, to provide a strong theoretical basis for the clinical treatment of heart failure with salsolinol.

Materials and methods

Bioinformatics tools. SwissTargetPrediction database (www.swisstargetprediction.ch) predicted that LSD1 was a potential target of salsolinol.

Patients and ethics. Serum from 15 patients with CHF (7 males and 8 females; age, 49-67; mean age 57.3±4.9 years) was collected at the Kunshan Hospital of Integrated Traditional Chinese and Western Medicine from April 2019 to September 2022. The present study was approved by the ethics committee of Kunshan Hospital of Integrated Traditional Chinese and Western Medicine (approval no. KY2021003) and a written consent form was signed by all participants prior to the experiments.

Cell culture. Human Cardiac fibroblasts (HCFs; cat. no. BNCC354381) were purchased from the BeNa Culture Collection and cultured in DMEM medium (Gibco; Thermo Fisher Scientific, Inc.) supplemented with 10% FBS (Gibco; Thermo Fisher Scientific, Inc.) at 37°C, in a humidified incubator supplied with 5% CO₂. When the cells grew to 50-60% confluence, the cells were pretreated with salsolinol (5, 10 or 20 µM; cat. no. 57256-34-5; purity: 99.86%; MedChemExpress) for 2 h and then treated with 100 nM angiotensin II (AngII; Sigma-Aldrich; Merck KGaA) for 48 h.

Cell proliferation assay. Cell proliferation was measured using a Cell Counting Kit-8 (CCK-8) assay kit (Beyotime Institute of Biotechnology) according to the manufacturer's instructions. Briefly, HCF cells were treated as above, after which 10 µl of CCK-8 solution was added and cells were incubated for 1 h. The absorbance at 450 nm was measured using a spectrophotometer.

EdU staining assay. An EdU staining kit (Beyotime Institute of Biotechnology) was used to analyze cell proliferation according to the manufacturer's protocol. Briefly, HCF cells were treated and then incubated with EdU (20 mmol/l) at 37°C for 2 h. The cells were fixed with 4% paraformaldehyde for 20 min at room temperature.

Wound healing assay. The treated HCF cells were cultured until they were ~90% confluent in six-well plates and then a scratch was created using a sterile 200 µl pipette tip.

Subsequently, cells were cultured in serum-free DMEM for 24 h. Images of the wounded area were taken after 0 and 24 h at the same microscopic cross point using a light microscope (Olympus Corporation). Wound width was measured using ImageJ version 1.52q (National Institutes of Health).

Immunofluorescence (IF) staining. After fixing the cells with 4% paraformaldehyde for 20 min at 4°C, the cells were washed and blocked for 1 h using 5% BSA (Gibco; Thermo Fisher Scientific, Inc.). Subsequently, cells were incubated overnight at 4°C with the primary α-smooth muscle actin (SMA) antibody (1:5,00; cat. no. orb311091; Biorbyt, Ltd.), after which cells were incubated with the secondary antibody for 1 h with a horseradish peroxidase-conjugated goat anti-rabbit secondary antibody (1:10,000; Abcam) at room temperature, followed by counterstaining with 5 µg/ml DAPI (Beyotime Institute of Biotechnology) for 2 min at 22°C. A fluorescence microscope (BXM1; Olympus Corporation) was used to visualize staining.

Western blotting. Total proteins were extracted from HCF cells using RIPA lysis buffer (Beyotime Institute of Biotechnology) and the protein concentration was quantified with a BCA assay kit (Beyotime Institute of Biotechnology). Equal amounts of proteins (20 µg per lane) were loaded on a 10% SDS-gel, resolved using SDS-PAGE and transferred to PVDF membranes (Invitrogen; Thermo Fisher Scientific, Inc.), after which, membranes were blocked with 5% BSA (Gibco; Thermo Fisher Scientific, Inc.) for 2 h at room temperature. The membranes were incubated with primary antibodies anti-Collagen I (1:1,000; cat. no. ab138492; Abcam), anti-Collagen III (1:1,000; cat. no. ab184993; Abcam), anti-α-SMA (1:1,000; cat. no. orb311091; Biorbyt, Ltd.), anti-LSD1 (1:1,000; cat. no. ab129195; Abcam), anti-phosphorylated (p)-STAT3 (1:1,000; cat. no. ab267373; Abcam), anti-STAT3 (1:1,000; cat. no. ab68153; Abcam), anti-Jagged-1 (1:1,000; cat. no. ab109536; Abcam), anti-NICD (1:1,000; cat. no. ab52627; Abcam), anti-GAPDH (1:1,000; cat. no. orb555879; Biorbyt, Ltd.) at 4°C overnight. The following day, membranes were incubated with HRP-conjugated anti-rabbit secondary antibodies (1:5,000; cat. no. ab7090; Abcam) for 1 h at room temperature. Signals were visualized using enhanced chemiluminescence reagent (MilliporeSigma) and ImageJ software 1.8.0 (National Institutes of Health) was used for the semi-quantification of protein density.

ELISA. The treated HCF cells were collected and then the concentrations of TNF-α (cat. no. H052-1-2) and IL-6 (cat. no. H007-1-2) were measured by the corresponding ELISA kits (Nanjing Jiancheng Bioengineering Institute) according to the manufacturer's instructions.

Detection of reactive oxygen species (ROS). The procedures of ROS measurement were according to manufacturer's instructions. The cells were incubated with 500 µl PBS containing 50 µM dichlorofluorescein diacetate (DCF-DA; cat. no. S0033; Beyotime Institute of Biotechnology) for 30 min at 37°C. Following three washes with PBS followed by centrifugation at 12,000 x g for 5 min at 4°C and DCF fluorescence intensity was detected using a BD FACS Calibur™ flow cytometer (BD Biosciences) at the excitation and emission wavelengths of 485

and 535 nm. BD CellQuest™ Pro software version 5.1 (BD Biosciences) was used to analyze ROS levels (11).

Molecular docking. The structure of salsolinol was drawn in the ChemDraw software (version 18.0) (12) and then imported into OpenBabel software (version 2.3.1) (13) for hydrogenation and converted into a mol2 format file. Subsequently, the structure of LSD1 (PDB ID: 2DW4) was obtained from the RCSB PDB (<https://www.rcsb.org/>). Thereafter, the protein LSD1 file was opened in PyMOL software (version 2.2.0) (14) to remove the excess water molecules, delete any irrelevant small ligands originally carried and to keep only the protein structure. As the downloaded protein structure had ligands, the original ligands were deleted and the original ligand positions were set as the docking sites. AutoDock (version 1.5.6) (14) was used to display the specific docking energy value after running. Finally, the results were analyzed with the adoption of Protein-Ligand Interaction Profiler (PLIP; <https://plip-tool.biotec.tu-dresden.de/plip-web>).

Reverse transcription-quantitative (RT-q) PCR. Total RNA was extracted from 1×10^4 HCF cells using TRIzol® reagent (Thermo Fisher Scientific, Inc.) according to the manufacturer's protocol. cDNA was synthesized from 1 µg total RNA using HIScript-II Q RT SuperMix for qPCR (Vazyme Biotech Co., Ltd.) according to the manufacturer's instructions. qPCR was performed and analyzed using the cDNA and SYBR Green PCR MasterMix (Nordic Bioscience) according to the manufacturer's instructions. The qPCR thermocycling conditions were: 40 cycles of 10 sec at 95°C and 20 sec at 60°C. Relative expression changes were calculated using the $2^{-\Delta\Delta C_q}$ method (15). LSD1 (KDM1A) forward and reverse primers were 5'-TGATCTTGGAGCCATGGTGG-3' and 5'-GACAGT GTCAGCTTGTCCGTT-3', GAPDH forward and reverse primers were 5'-AATGGGCAGCCGTTAGGAAA-3' and 5'-GCGCCCAATACGACCAAATC-3'. The experiments were replicated three times.

Cell transfection. The LSD1 overexpression vector (Ov-LSD1) was established by inserting the LSD1 gene into the pcDNA3.1 vector (Shanghai GeneChem Co., Ltd.), whereas an empty vector served as the negative control (Ov-NC). Then, HCF cells in the 2nd generation system were inoculated into 6-well plates at a density of 2×10^5 cells/well and cultured until cell confluence has reached 80%. After that, a total of 100 nM plasmids were transfected into HCF cells at 37°C for 48 h using Lipofectamine® 2000 transfection reagent (Invitrogen; Thermo Fisher Scientific, Inc.) according to the manufacturer's protocol. HCF cells were infected using a retroviral supernatant (6×10^8 TU/ml) for 72 h, then treated with 0.5 µg/ml puromycin for 2 weeks to obtain stably transfected cells. After transfection for 48 h, the transfection efficiency was detected using RT-qPCR and western blotting according to the aforementioned methods.

Statistical analysis. Data are presented as the mean ± standard deviation and were analyzed using a one-way ANOVA followed by a Tukey's post hoc test in SPSS version 16.0 (SPSS, Inc.). The normal distribution of variables was assessed by the Shapiro-Wilk test. $P < 0.05$ was considered to indicate a statistically significant difference.

Results

Salsolinol inhibits the proliferation and migration of AngII-induced HCFs. Different concentrations (5, 10, or 20 µM) of salsolinol were used to treat HCFs and a CCK-8 assay was used to detect cell viability. The results showed that 5, 10 and 20 µM salsolinol did not have a noticeable toxic effect (Fig. 1A). The cells were then divided into a control, AngII, AngII + 5 µM, AngII + 10 µM and AngII + 20 µM groups. The results of the CCK-8 and EdU staining assays showed increased cell proliferation in the AngII group compared with the control group. However, different concentrations of salsolinol reduced cell viability in a concentration-dependent manner (Fig. 1B and C). The cell migratory ability was detected using a wound healing assay and the results showed that the migratory ability was significantly increased following AngII induction compared with the control group. Salsolinol significantly inhibited HCF migration (Fig. 1D).

Salsolinol inhibits AngII-induced HCF fibrosis. The expression of α-SMA was detected using an IF assay. The results showed that α-SMA expression in the AngII group was significantly higher than that in the control group; salsolinol inhibited this increase in a dose-dependent manner (Fig. 2A). Western blotting was used to detect the expression of fibrosis-related proteins α-SMA, Collagen I and Collagen III and the results showed that AngII significantly increased the expression of these proteins in cells. Salsolinol inhibited this increase in a dose-dependent manner (Fig. 2B).

Salsolinol inhibits inflammation and ROS production in AngII-induced HCFs. Subsequently, the expression of cytokines related to inflammation was detected and the results of ELISA showed that compared with the control group, the expression of TNF-α and IL-6 were significantly increased in the AngII group, while salsolinol dose-dependently reduced the expression of TNF-α and IL-6 compared with the AngII group (Fig. 3A). AngII induced an increase in ROS expression in the cells, while salsolinol inhibited this increase in a dose-dependent manner (Fig. 3B).

Salsolinol inhibits LSD1 expression and regulates the STAT3/Notch-1 signaling pathway. As predicted by SwissTargetPrediction database, LSD1 was a potential target of salsolinol. Using serum from patients with CHF, it was found that LSD1 expression was significantly increased in patients with CHF compared with the control group (Fig. 4A). In the *in vitro* experiments, western blotting was used to detect the expression of LSD1 and proteins associated with the STAT3/Notch-1 signaling pathway. Compared with the control group, the expression of LSD1 was increased in the AngII group. The expression of p-STAT3 was increased, while the expression of Jagged-1 and NICD proteins was significantly decreased in the AngII group. Administration of salsolinol reversed the changes in the expression of these proteins in a dose-dependent manner (Fig. 4B). Molecular docking analysis showed that salsolinol could target and regulate the expression of LSD1 (Fig. 4C). Therefore, it was concluded that salsolinol inhibited LSD1 and regulated the STAT3/Notch-1 signaling pathway.

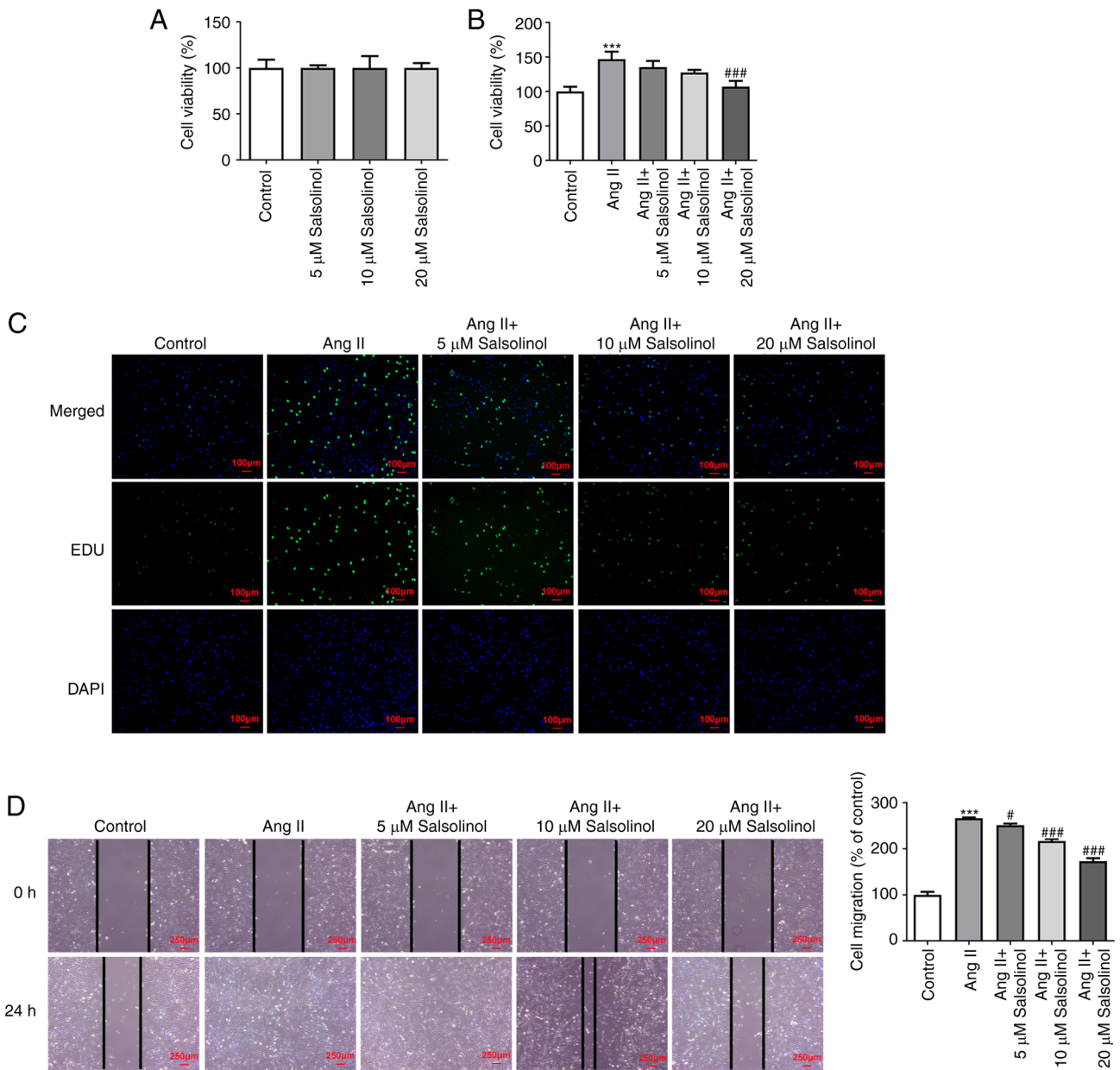


Figure 1. Salsolinol inhibits hyperproliferation and migration in AngII-induced HCFs. (A) Different concentrations (5, 10 and 20 μ M) of salsolinol were applied to HCFs and CCK8 was used to detect cell viability. The cells were then divided into control, AngII, AngII + 5 μ M, AngII + 10 μ M and AngII + 20 μ M groups. (B) CCK8 and (C) EdU staining were used to detect cell proliferation. (D) The cell migration ability was detected by cell scratch assay. ^{***} $P < 0.001$ vs. Control; [#] $P < 0.05$, ^{###} $P < 0.001$ vs. AngII. AngII, angiotensin II; HCFs, human cardiac fibroblasts.

Upregulation of LSD1 reverses the effect of salsolinol on AngII-induced HCFs. An LSD1 overexpression cell line was constructed and transfection efficiency was detected using RT-qPCR and western blotting (Fig. 5A and B); 20 μ M salsolinol was selected for follow-up experiments. Cells were divided into a control, AngII, AngII + salsolinol, AngII + salsolinol + Ov-NC and AngII + salsolinol + Ov-LSD1 groups. EdU staining results showed that compared with the AngII + salsolinol + Ov-NC group, the proliferative ability of AngII + salsolinol + Ov-LSD1 group was increased (Fig. 5C). The results of the wound healing assay showed that overexpression of LSD1 significantly reversed the increase in cell migration induced by salsolinol (Fig. 5D). The results of IF and western blotting showed that compared with the AngII + salsolinol + Ov-NC group, the expression of α -SMA, Collagen

I and Collagen III in the AngII + Salsolinol + Ov-LSD1 group was increased (Fig. 6A and B). The results of ELISA showed that overexpression of LSD1 significantly reversed the inhibition of TNF- α , IL-6 and ROS by salsolinol (Fig. 6C and D).

Discussion

Patients with CHF have relatively poor cardiac function and the myocardial interstitium also presents in an abnormal state during the occurrence and development of the disease, leading to the relative disorder of the myocardial structure (16). Several studies have shown that the above factors can lead to myocardial fibrosis and thus lead to abnormal cardiac function (17,18). In addition, myocardial fibrosis is a common pathological manifestation of the majority of

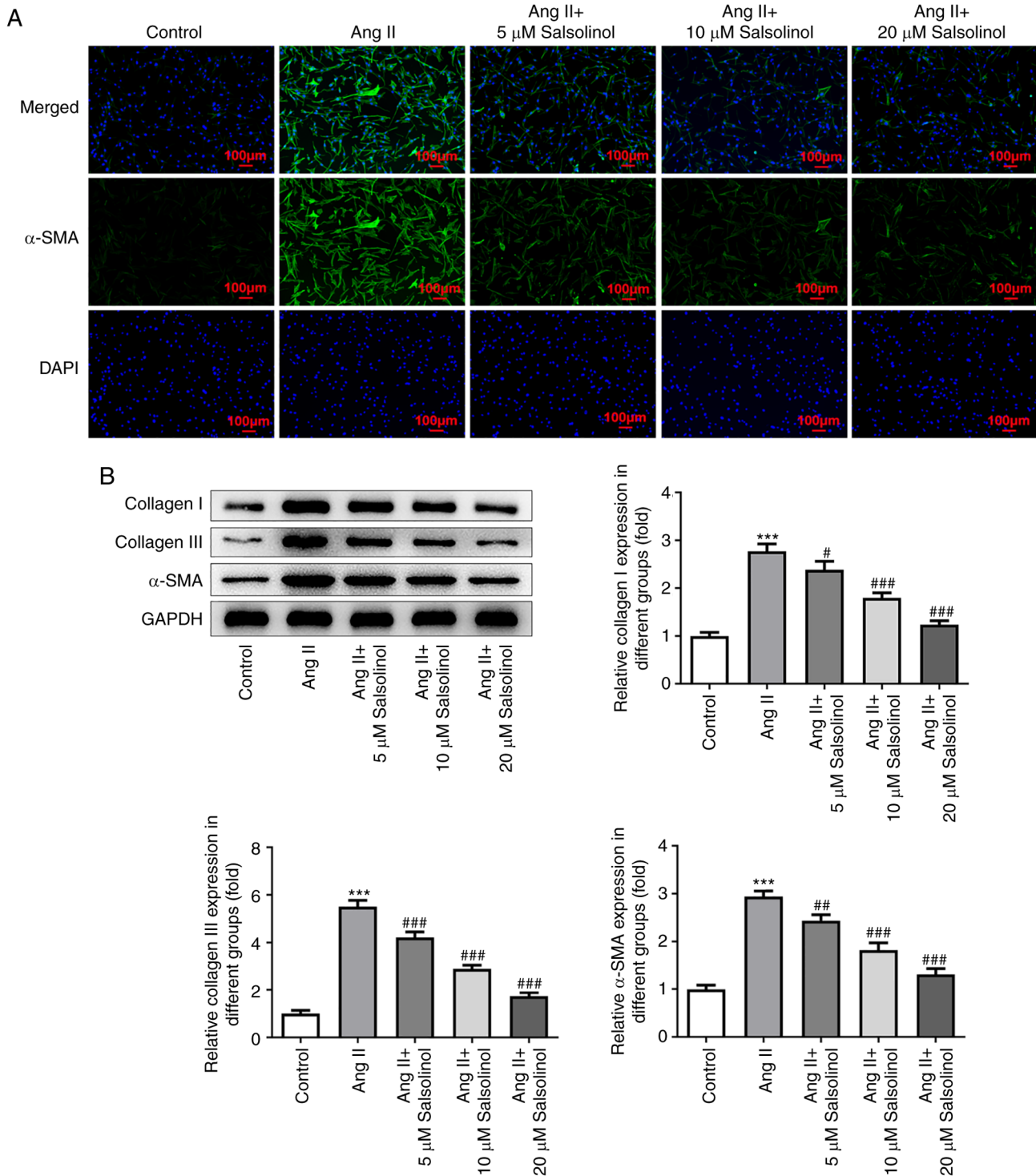


Figure 2. Salsolinol inhibits AngII-induced HCFs fibrosis. (A) The expression of α -SMA was detected by immunofluorescence assay. (B) Western blotting detected the expressions of fibrosis related proteins α -SMA, Collagen I and III. ^{***} P <0.001 vs. Control; [#] P <0.05, ^{##} P <0.01 and ^{###} P <0.001 vs. AngII. AngII, angiotensin II; HCFs, human cardiac fibroblasts; α -SMA, α -smooth muscle actin.

heart diseases, which leads to heart failure and arrhythmia caused by changes in the electrical conduction of the heart. Therefore, it is necessary to study the changes of myocardial fibrosis in these patients.

Cardiac fibroblasts are the most abundant type of cells in the heart that respectively account for ~27, ~64 and ~72% of the heart mass in mice, rats and humans and are the key cell type responsible for maintaining the structural integrity of the

heart (19). In a pathological state, fibroblasts are activated to transform into myofibroblasts, which have higher contractility and mobility, stronger ability to synthesize extracellular matrix proteins and the expression of several marker proteins such as α -SMA in these cells is significantly upregulated (20,21). Phenotypic changes of cardiac fibroblasts in cardiovascular diseases and a series of functional changes following these changes are the basis of myocardial fibrosis (22). In the present

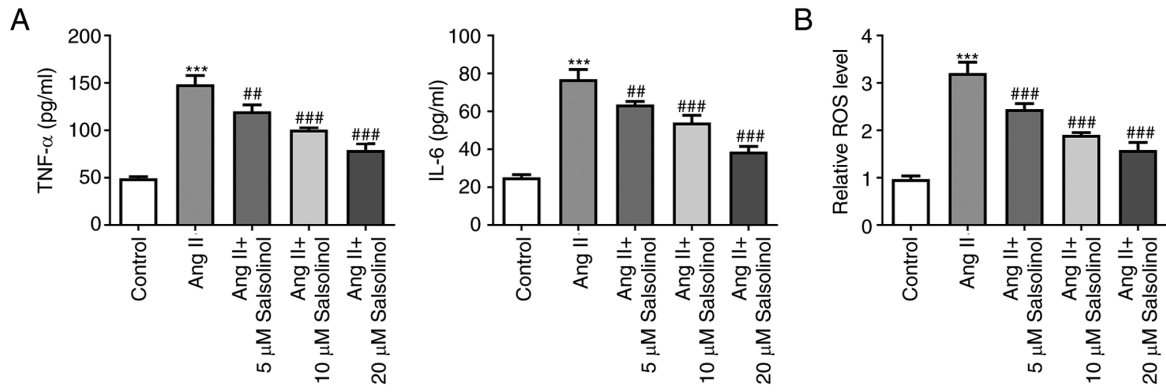


Figure 3. Salsolinol inhibits inflammation and ROS production in AngII-induced HCFs. (A) The expression of cytokines related to inflammation was detected by ELISA. (B) ROS expression was detected by a kit. ***P<0.001 vs. Control; **P<0.01, ***P<0.001 vs. AngII. ROS, reactive oxygen species; AngII, angiotensin II; HCFs, human cardiac fibroblasts.

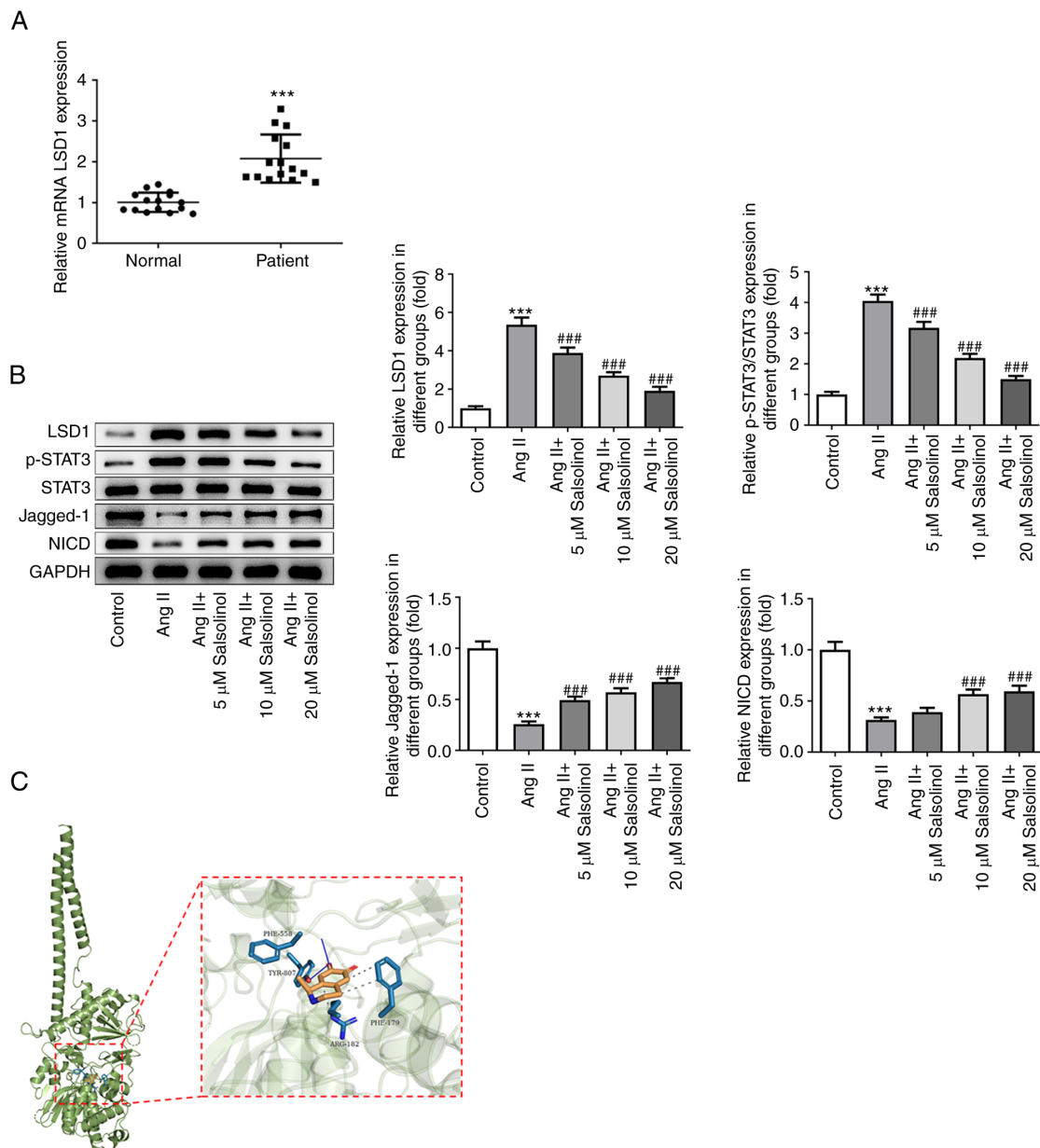


Figure 4. Salsolinol inhibits LSD1 expression and then regulates STAT3/Notch-1 signaling pathway. (A) Reverse transcription-quantitative PCR was used to detect the LSD1 expression in the serum in patients with CHF. (B) Western blot was used to detect the expressions of LSD1 and the proteins related to the STAT3/Notch-1 signaling pathway. (C) Molecular docking techniques predicted the relationship between salsolinol and LSD1. ***P<0.001 vs. Control; ***P<0.001 vs. AngII. LSD1, lysine-specific histone demethylase 1A; CHF, congestive heart failure; AngII, angiotensin II; p-, phosphorylated.

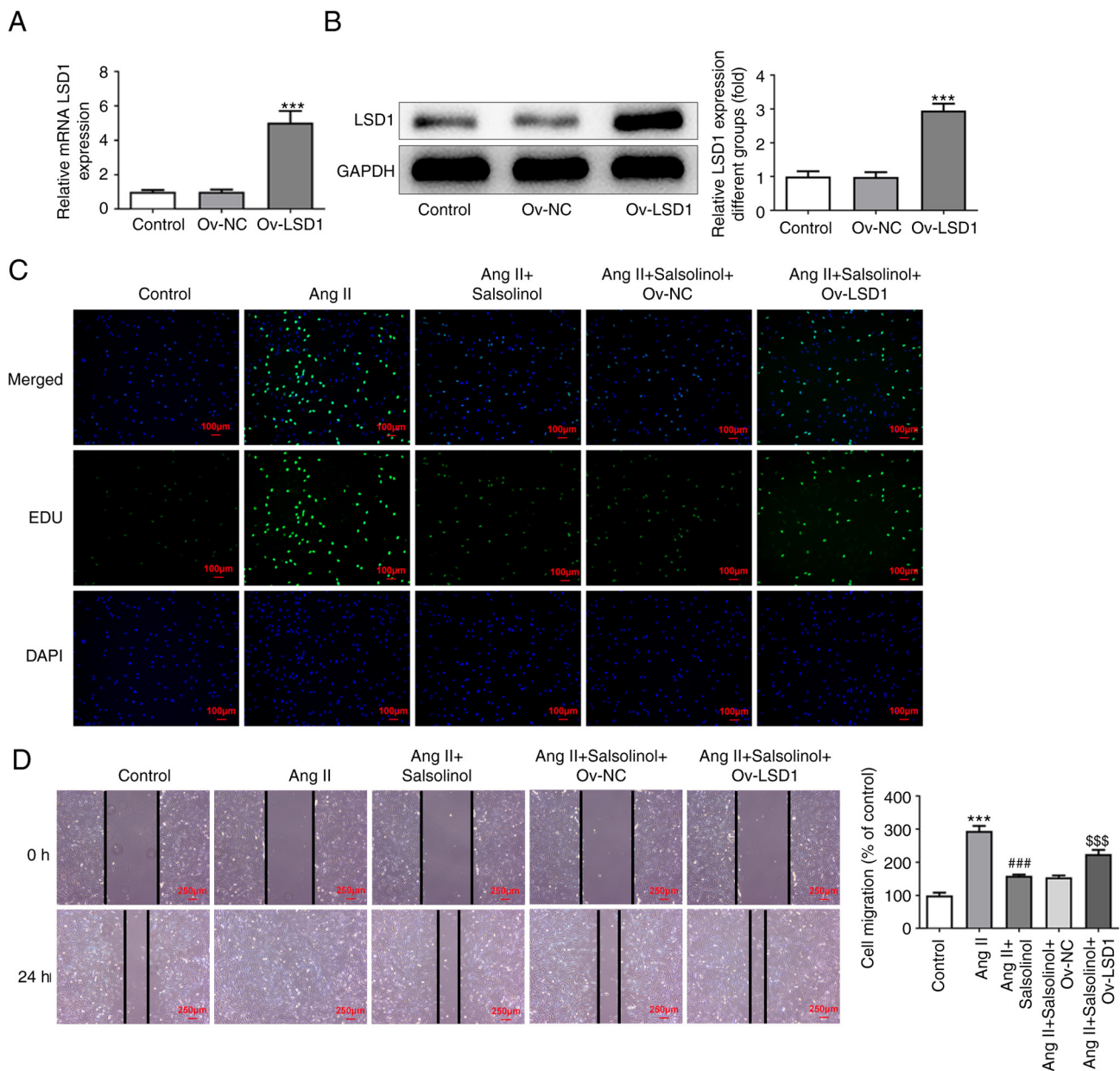


Figure 5. Upregulation of LSD1 reverses the effect of salsolinol on AngII-induced HCFs. LSD1 overexpression plasmid was constructed and transfection efficiency was detected by (A) reverse transcription-quantitative PCR and (B) western blotting. *** $P < 0.001$ vs. Ov-NC. (C) EdU staining was used to detect cell proliferation. (D) The cell migration ability was detected by cell scratch assay. *** $P < 0.001$ vs. Control; ### $P < 0.001$ vs. AngII; \$\$\$ $P < 0.001$ vs. AngII + Salsolinol + Ov-NC. AngII, lysine-specific histone demethylase 1A; AngII, angiotensin II; HCFs, human cardiac fibroblasts; NC, negative control.

study, HCFs were used for experimentation and AngII was used to induce HCFs as a model of cardiac fibrosis.

At present, there are few clinical methods for the treatment of myocardial fibrosis and those that do exist have limited effects. Research has found that certain types of traditional Chinese medicines can improve heart failure through an anti-cardiac fibrosis effect and this research direction has gradually garnered increasing interest (1). Research has shown that salsolinol, a chemical present in the popular prescription Ershen Zhenwu Decoction (ESZWD) has potential for treating heart failure with what is termed in traditional Chinese medicine heart-kidney Yang deficiency syndrome (23). Water soluble alkaloids of aconitum have a significant therapeutic effect on acute heart failure rats and salsolinol is a biological component of the water-soluble alkaloids present in aconitum,

suggesting that salsolinol may have a therapeutic effect on acute heart failure (4). Salsolinol regulates angiotensin-converting enzyme, which serves an important role in improving chronic myocardial ischemia (24). However, whether salsolinol has a therapeutic effect on myocardial fibrosis in CHF has not been reported. In the present study, salsolinol was shown to exhibit no significant cytotoxic effects on HCFs. In addition, it significantly inhibited the abnormal proliferation and migration of HCFs in a dose dependent manner. Salsolinol significantly inhibited the expression of fibrosis-related proteins α -SMA, Collagen I and Collagen III, the expression of inflammatory factors TNF- α and IL-6 and the generation of oxidative stress factor ROS in a dose dependent manner. It indicated that salsolinol inhibited fibrotic effect of HCFs as well as the cellular inflammatory and oxidative stress responses in a dose-dependent manner. A previous

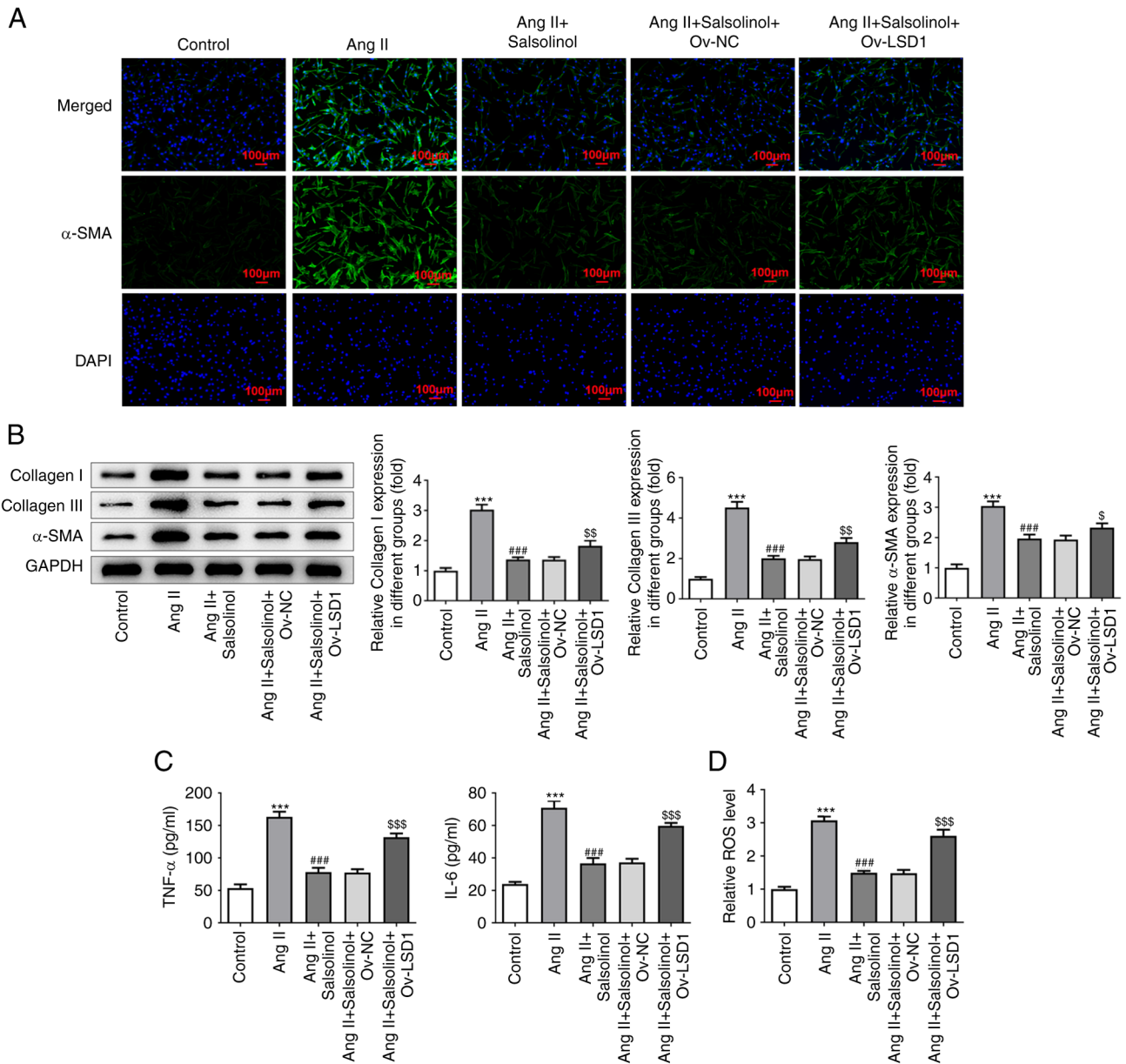


Figure 6. Upregulation of LSD1 reverses the effect of salsolinol on AngII-induced HCFs. (A) The expression of α -SMA was detected by immunofluorescence assay. (B) Western blotting detected the expressions of fibrosis related proteins α -SMA, Collagen I and III. (C) The expression of cytokines related to inflammation was detected by ELISA. (D) ROS expression was detected by a kit. *** $P < 0.001$ vs. Control; ### $P < 0.001$ vs. AngII; $^{\#}P < 0.05$, $^{SS}P < 0.01$, $^{SSS}P < 0.001$ vs. AngII + Salsolinol + Ov-NC. LSD1, lysine-specific histone demethylase 1A; AngII, angiotensin II; HCFs, human cardiac fibroblasts; α -SMA, α -smooth muscle actin; ROS, reactive oxygen species; NC, negative control.

study has shown that salsolinol has obvious cardiotoxic and anti-inflammatory effects (5). This is consistent with the results of salsolinol on anti-inflammatory and antioxidant stress of HCFs in the present study.

Next, the specific regulatory mechanism of the effects of salsolinol on HCFs was determined. Using molecular docking analysis, it was found that salsolinol could dock with LSD1. In addition, it was found that LSD1 expression was abnormally elevated in the serum of CHF patients and AngII-induced HCFs. A previous study showed increased expression of LSD1 in the kidney of mice with unilateral ureteral obstruction and TGF- β 1-induced NRK-52E cells and inhibition of LSD1 using a specific inhibitor, ORY1001, alleviated renal epithelial-to-mesenchymal transition and fibrosis (25). In

bleomycin-induced pulmonary fibrosis mice and lung tissues of TGF- β 1-treated lung fibroblasts, LSD1 expression was elevated and LSD1 activation promoted differentiation and fibrosis of lung myoblasts by targeting the TGF- β 1/Smad3 signaling pathway (26). These results indicated that LSD1 served an important regulatory role in tissue fibrosis. In addition, LSD1 deficiency in myofibroblasts has been shown to alleviate heart failure in mice. The results of the present study showed that upregulation of LSD1 reversed the effects of salsolinol on AngII-induced HCF proliferation, migration, inflammatory response and fibrosis.

A previous study showed that LSD1 induced epithelial interstitial transformation and promoted renal fibrosis through the Jagged-1/Notch signaling pathway (27). TRIM72

promoted cardiac fibrosis via regulation of the STAT3/Notch-1 signaling (28). PKM2 can also promote AngII-induced cardiac remodeling via activation of the TGF- β /Smad2/3 and Jak2/Stat3 pathways via oxidative stress (29). Feverolin, an inhibitor of the STAT3 signaling pathway, attenuates AngII-induced left ventricular hypertrophy via regulation of fibroblast activity (30). Therefore, it is reasonable to hypothesize that LSD1 can regulate the downstream pathway STAT3/Notch-1 following salsolinol-mediated regulation of LSD1, thereby inhibiting myocardial fibrosis. The results of the present study showed that following AngII induction of HCFs, p-STAT3 expression was activated and Jagged-1 and NICD expression were inhibited in cells. The expression of the members of the STAT3/Notch-1 signaling pathway was reversed following salsolinol treatment of AngII-induced HCFs. Therefore, it was preliminarily concluded that salsolinol inhibited LSD1 via regulation of the STAT3/Notch-1 signaling pathway to improve AngII-induced myocardial fibrosis *in vitro*. However, whether this mechanism is observed *in vivo* remains to be determined and thus serves as a limitation of the present study. In addition, there is another limitation to the present study, that is, it only detected the expression level of LSD1 protein in patients' blood and the expression level of LSD1 protein in patient tissues will be detected in the future experiments.

In conclusion, salsolinol inhibited LSD1 via regulation of the STAT3/Notch-1 signaling pathway to improve AngII-induced myocardial fibrosis *in vitro*. The results of the present study provide a theoretical basis for the clinical treatment of CHF with salsolinol. However, *in vivo* experiments and clinical investigations should be performed to verify the mechanism of salsolinol pair against specific types of cancer in future studies.

Acknowledgements

Not applicable.

Funding

The present study was supported by the 2019 Kunshan Key Research and Development Plan Social Development Project (grant no. KS1915), the 2021 Suzhou Science and Technology Development Plan (grant no. SKJYD2021206), the 2022 Kunshan Key Research and Development Plan Social Development Project (grant no. KSZ2212) and the Suzhou Science and Technology Development Plan Project (grant no. SKYXD2022069).

Availability of data and materials

The data sets generated and/or analyzed during the present study are available from the corresponding author on reasonable request.

Authors' contributions

JW designed and conceived the present study. XZ, ZS, YN, FC and XY performed the experiments and wrote the manuscript. JW, XZ and ZS performed the data analysis. YN and FC confirmed the authenticity of all the raw data. All authors have read and approved the final manuscript.

Ethics approval and consent to participate

The present study was approved by the ethics committee of Kunshan Hospital of Integrated Traditional Chinese and Western Medicine (approval no. KY2021003) and informed consent was obtained from patients prior to beginning the experiments.

Patient consent for publication

Not applicable.

Competing interests

The authors declare that they have no competing interests.

References

- Kennelly P, Sapkota R, Azhar M, Cheema FH, Conway C and Hameed A: Diuretic therapy in congestive heart failure. *Acta Cardiol* 77: 97-104, 2022.
- Abdelbasset WK and Alqahtani BA: A randomized controlled trial on the impact of moderate-intensity continuous aerobic exercise on the depression status of middle-aged patients with congestive heart failure. *Medicine (Baltimore)* 98: e15344, 2019.
- Wen J, Li M, Zhang W, Wang H, Bai Y, Hao J, Liu C, Deng K and Zhao Y: Role of higenamine in heart diseases: A mini-review. *Front Pharmacol* 12: 798495, 2022.
- Liu M, Li Y, Tang Y, Zheng L and Peng C: Synergistic effect of aconiti lateralis radix praeparata water-soluble alkaloids and ginseng radix et rhizoma total ginsenosides compatibility on acute heart failure rats. *J Chromatogr B Analyt Technol Biomed Life Sci* 1137: 121935, 2020.
- Xu X, Xie X, Zhang H, Wang P, Li G, Chen J, Chen G, Cao X, Xiong L, Peng F and Peng C: Water-soluble alkaloids extracted from aconiti lateralis praeparata protect against chronic heart failure in rats via a calcium signaling pathway. *Biomed Pharmacother* 135: 111184, 2021.
- Yang Y, Hu P, Zhou X, Wu P, Si X, Lu B, Zhu Y and Xia Y: Transcriptome analysis of aconitum carmichaelii and exploration of the salsolinol biosynthetic pathway. *Fitoterapia* 140: 104412, 2020.
- Wen J, Zhang L, Liu H, Wang J, Li J, Yang Y, Wang Y, Cai H, Li R and Zhao Y: Salsolinol attenuates doxorubicin-induced chronic heart failure in rats and improves mitochondrial function in H9c2 cardiomyocytes. *Front Pharmacol* 10: 1135, 2019.
- Zhang S, Liu M, Yao Y, Yu B and Liu H: Targeting LSD1 for acute myeloid leukemia (AML) treatment. *Pharmacol Res* 164: 105335, 2021.
- Guenantin AC, Jebeniani I, Leschik J, Watrin E, Bonne G, Vignier N and Puc  at M: Targeting the histone demethylase LSD1 prevents cardiomyopathy in a mouse model of laminopathy. *J Clin Invest* 131: e136488, 2021.
- Huo JL, Jiao L, An Q, Chen X, Qi Y, Wei B, Zheng Y, Shi X, Gao E, Liu HM, *et al*: Myofibroblast deficiency of LSD1 alleviates TAC-induced heart failure. *Circ Res* 129: 400-413, 2021.
- Bao J, Ye C, Zheng Z and Zhou Z: Fmr1 protects cardiomyocytes against lipopolysaccharide-induced myocardial injury. *Exp Ther Med* 16: 1825-1833, 2018.
- Evans DA: History of the harvard ChemDraw project. *Angew Chem Int Ed Engl* 53: 11140-11145, 2014.
- Lin Z, Zhang Z, Ye X, Zhu M, Li Z, Chen Y and Huang S: Based on network pharmacology and molecular docking to predict the mechanism of Huangqi in the treatment of castration-resistant prostate cancer. *PLoS One* 17: e0263291, 2022.
- Zhang Y, Liu X, Long J, Cheng X, Wang X and Feng X: Exploring active compounds and mechanisms of angong niuhuang wan on ischemic stroke based on network pharmacology and molecular docking. *Evid Based Complement Alternat Med* 2022: 2443615, 2022.
- Livak KJ and Schmittgen TD: Analysis of relative gene expression data using real-time quantitative PCR and the 2(-Delta Delta C(T)) method. *Methods* 25: 402-408, 2001.

16. Yu H, Basu S and Hallow KM: Cardiac and renal function interactions in heart failure with reduced ejection fraction: A mathematical modeling analysis. *PLoS Comput Biol* 16: e1008074, 2020.
17. González A, Schelbert EB, Diez J and Butler J: Myocardial interstitial fibrosis in heart failure: Biological and translational perspectives. *J Am Coll Cardiol* 71: 1696-1706, 2018.
18. Rao M, Wang X, Guo G, Wang L, Chen S, Yin P, Chen K, Chen L, Zhang Z, Chen X, *et al*: Resolving the intertwining of inflammation and fibrosis in human heart failure at single-cell level. *Basic Res Cardiol* 116: 55, 2021.
19. Kurose H: Cardiac fibrosis and fibroblasts. *Cells* 10: 1716, 2021.
20. Tallquist MD: Cardiac fibroblast diversity. *Annu Rev Physiol* 82: 63-78, 2020.
21. Liu M, López de Juan Abad B and Cheng K: Cardiac fibrosis: Myofibroblast-mediated pathological regulation and drug delivery strategies. *Adv Drug Deliv Rev* 173: 504-519, 2021.
22. Maruyama K and Imanaka-Yoshida K: The pathogenesis of cardiac fibrosis: A review of recent progress. *Int J Mol Sci* 23: 2617, 2022.
23. Hong LL, Zhao Y, Chen WD, Yang CY, Li GZ, Wang HS and Cheng XY: Tentative exploration of pharmacodynamic substances: Pharmacological effects, chemical compositions, and multi-components pharmacokinetic characteristics of ESZWD in CHF-HKYd rats. *Front Cardiovasc Med* 9: 913661, 2022.
24. Guo S, Li P, Fu B, Chuo W, Gao K, Zhang W, Wang J, Chen J and Wang W: Systems-biology dissection of mechanisms and chemical basis of herbal formula in treating chronic myocardial ischemia. *Pharmacol Res* 114: 196-208, 2016.
25. Zhang X, Li LX, Yu C, Nath KA, Zhuang S and Li X: Targeting lysine-specific demethylase 1A inhibits renal epithelial-mesenchymal transition and attenuates renal fibrosis. *FASEB J* 36: e22122, 2022.
26. Pan X, Li J, Tu X, Wu C, Liu H, Luo Y, Dong X, Li X, Pan LL and Sun J: Lysine-specific demethylase-1 regulates fibroblast activation in pulmonary fibrosis via TGF- β 1/Smad3 pathway. *Pharmacol Res* 152: 104592, 2020.
27. Zhang H, Xing J and Zhao L: Lysine-specific demethylase 1 induced epithelial-mesenchymal transition and promoted renal fibrosis through Jagged-1/Notch signaling pathway. *Hum Exp Toxicol* 40 (12 Suppl): S203-S214, 2021.
28. Chen X, Su J, Feng J, Cheng L, Li Q, Qiu C and Zheng Q: TRIM72 contributes to cardiac fibrosis via regulating STAT3/Notch-1 signaling. *J Cell Physiol* 234: 17749-17756, 2019.
29. Zhang X, Zheng C, Gao Z, Wang L, Chen C, Zheng Y and Meng Y: PKM2 promotes angiotensin-II-induced cardiac remodelling by activating TGF- β /Smad2/3 and Jak2/Stat3 pathways through oxidative stress. *J Cell Mol Med* 25: 10711-10723, 2021.
30. Skoumal R, Tóth M, Serpi R, Rysä J, Leskinen H, Ulvila J, Saiho T, Aro J, Ruskoaho H, Szokodi I and Kerkelä R: Parthenolide inhibits STAT3 signaling and attenuates angiotensin II-induced left ventricular hypertrophy via modulation of fibroblast activity. *J Mol Cell Cardiol* 50: 634-641, 2011.



Copyright © 2023 Zhang et al. This work is licensed under a Creative Commons Attribution-NonCommercial-NoDerivatives 4.0 International (CC BY-NC-ND 4.0) License.